Experimental Cell Research 442 (2024) 114211

Contents lists available at ScienceDirect

Experimental Cell Research

journal homepage: www.elsevier.com/locate/yexcr

Research article

Vascular smooth muscle cell-derived exosomes promote osteoblast-to-osteocyte transition via β-catenin signaling

Célio J.C. Fernandes [a], Rodrigo A. Silva [b], Marcel R. Ferreira [a], Gwenny M. Fuhler [c], Maikel P. Peppelenbosch [c], Bram CJ. van der Eerden [d], Willian F. Zambuzzi [a,*]

[a] Bioassays and Cell Dynamics Lab, Dept. of Chemistry and Biochemistry, Bioscience Institute, UNESP, Botucatu, 18603-100, Sao Paulo, Brazil
[b] School of Dentistry, University of Taubaté, 12020-340, Taubaté, São Paulo, Brazil
[c] Department of Gastroenterology and Hepatology, Erasmus MC, Erasmus University Medical Center, Dr Molewaterplein 40, 3015 GD, Rotterdam, the Netherlands
[d] Department of Internal Medicine, Erasmus MC, Erasmus University Medical Center, Dr Molewaterplein 40, 3015 GD, Rotterdam, the Netherlands

A B S T R A C T

Blood vessel growth and osteogenesis in the skeletal system are coupled; however, fundamental aspects of vascular function in osteoblast-to-osteocyte transition remain unclear. Our study demonstrates that vascular smooth muscle cells (VSMCs), but not endothelial cells, are sufficient to drive bone marrow mesenchymal stromal cell-derived osteoblast-to-osteocyte transition via β-catenin signaling and exosome-mediated communication. We found that VSMC-derived exosomes are loaded with transcripts encoding proteins associated with the osteocyte phenotype and members of the WNT/β-catenin signaling pathway. In contrast, endothelial cell-derived exosomes facilitated mature osteoblast differentiation by reprogramming the TGFB1 gene family and osteogenic transcription factors osterix (SP7) and RUNX2. Notably, VSMCs express significant levels of tetraspanins (CD9, CD63, and CD81) and drive the intracellular trafficking of exosomes with a lower membrane zeta potential than those from other cells. Additionally, the high ATP content within these exosomes supports mineralization mechanisms, as ATP is a substrate for alkaline phosphatase. Osteocyte function was further validated by RNA sequencing, revealing activity in genes related to intermittent mineralization and sonic hedgehog signaling, alongside a significant increase in TNFSF11 levels. Our findings unveil a novel role of VSMCs in promoting osteoblast-to-osteocyte transition, thus offering new insights into bone biology and homeostasis, as well as in bone-related diseases. Clinically, these insights could pave the way for innovative therapeutic strategies targeting VSMC-derived exosome pathways to treat bone-related disorders such as osteoporosis. By manipulating these signaling pathways, it may be possible to enhance bone regeneration and improve skeletal health in patients with compromised bone structure and function.

1. Introduction

Bone needs to continuously remodel throughout life to maintain optimal mineral homeostasis and structural integrity. This remodeling process involves several sequential steps referred to as the activation-resorption-formation cycle [1] and culminates in a strict balance between osteoblasts and bone-resorbing osteoclasts to avoid bone loss. Despite their central role in bone remodeling and health, the development of osteocytes has received remarkably little attention. Unlike osteoblast development, little is known about the molecular and transcriptional regulators able to drive osteoblast-to-osteocyte transition [2]. Osteocytes, comprising over 95 % of all bone cells [3], have long been seen as quiescent cells trapped within the compact bone, leading to an underestimation of their role in bone homeostasis [4]. Additionally, these cells are challenging to study due to their limited accessibility in vitro and in vivo.

Osteocytes are suggested to function as mechanosensors, releasing anabolic signals including nitric oxide (NO), prostaglandins, and ATP [5]. ATP is speculated to be a decisive factor during the intermittent mineralization process by serving as a phosphate donor for alkaline phosphatase (ALPL) activity. NO, a short-lived free radical, inhibits bone resorption and promotes bone formation in response to mechanical strain [6,7]. NO also promotes angiogenesis [8,9], with studies by Adams et al. highlighting the dynamic activity of endothelial cells on bone formation and homeostasis by establishing an intricate molecular framework coupling angiogenesis, angiocrine signals, and osteogenesis [10], also considering the role of vascular smooth muscle cells (VSMCs) in controlling blood flow, which can impact bone health [11].

Although several studies have demonstrated that bone formation processes are coupled to angiogenesis [12], the relevance of VSMCs in this scenario is barely known. Therefore, we investigated the effect of VSMCs and their products on osteoblast-to-osteocyte transition, primarily considering exosomes and their cargo as principal players in driving this coupling. Our hypothesis was addressed using modern methodologies, and the data are sufficient to propose a mechanism involving the crosstalk between VSMCs and osteoblasts, considering the

* Corresponding author.
E-mail address: w.zambuzzi@unesp.br (W.F. Zambuzzi).

https://doi.org/10.1016/j.yexcr.2024.114211
Received 26 June 2024; Received in revised form 1 August 2024; Accepted 13 August 2024
Available online 14 August 2024

involvement of microRNAs and osteocyte-related markers. This study enhances our understanding of the complex communication between bone cells and blood vessels, which is necessary for developing novel therapies for bone-related disorders such as osteoporosis and osteogenesis imperfecta. However, it is important to acknowledge the limitations of our study. The major exploration of the data focused on identifying gene expression as a methodology to confirm the phenotype of the cells. While gene expression analysis is a powerful tool, it requires complementary validation at the protein and functional levels to fully establish the observed phenotypes. Future studies should aim to include such validations to strengthen the conclusions drawn from gene expression data.

2. Material & methods

2.1. Cell culture

All cells were maintained at conventional conditions, exactly as recommended by the manufacturers. The vascular cells were purchased from LONZA (Alpharetta, GA, USA): a_EC – Human Coronary Artery Endothelial Cells (Catalog #: CC-2585), v_EC – Human Umbilical Vein Endothelial Cells, Single Donor (Catalog #: CC-2517), and VSMC – Human Aortic Smooth Muscle Cells (Catalog #: CC-2571; in this study named VSMCs). Human osteoblasts derived from bone of healthy donors undergoing joint work at Fluminense Federal University - cells were collected from bone explants during orthopedic surgeries. The procedure was approved by the local Ethics Committee, Fluminense Federal University (protocol # 232/08). As a positive control, those osteoblasts were subjected to osteogenic medium (O.M.) containing β-glycerophosphate (10 mM; G9422, Sigma-Aldrich; St. Louis, MO, USA) + dexamethasone (0.03 g/mL; D4902, Sigma-Aldrich; St. Louis, MO, USA) + ascorbic acid (50 μg/mL; A5960, Sigma-Aldrich; St. Louis, MO, USA), and the in vitro mineralization was analyzed by Alizarin RedS (A5533-25G; Sigma-Aldrich; St. Louis, MO, USA) Staining. The experimental design is shown schematically (Fig. S1).

2.2. Laser confocal microscopy

For confocal microscopy analysis, the cells were cultured in glass coverslips, as we have reported previously[13–16].

Sample preparation for qPCR. To collect samples for qPCR technology, we have performed the TRIzol (15596026, Thermo Fisher Scientific, Waltham, MA USA) methodology, exactly as recommended by the manufacturer. Results were expressed as relative amounts of the transcripts with GAPDH as reference gene (housekeeping gene), using the comparative CT method (ΔΔCt)[17]. Primers and details are described in Table 1.

2.3. Isolation of exosomes and characterization

For analysis and exosomes [18], the culture medium was supplemented with extracellular vesicles from Free Fetal Serum, performed using ultracentrifugation at 30,000×*g* for 18 h [19–21]. Cells remained for 72 h with EVs-free cell culture medium, Static, or Shear-Stress, after which the medium was removed and used to isolate exosomes with the Total Exosome Isolation Reagent (from cell culture media; 4478359, Thermo Fisher Scientific, Waltham, MA USA) according to the manufacturer's instructions. The exosomes were examined using the Tecnai Spirit Electronic Transmission Microscope. NanoSight NS300 (Amesbury, UK) was used to determine the size and concentration of exosomes that perform nanoparticle tracing analysis based on light scattering and Brownian motion properties of the samples, and the Malvern Zetasizer Nano ZS instrument was used to measure zeta potential. Exosome markers analysis (anti-CD9, cat. number 563641; anti-CD63 cat. number 556019; and anti-CD81 cat. number 555675, were purchased from BD Bioscience, New Jersey, USA) was performed using FACS. To measure ATP, the exosomes were boiled at 45 °C for 2 min and dosing was performed according to the instructions of the CellTiter-Glo® Luminescent Cell Viability Assay Technical Bulletin Kit (Promega, Madison, WI, USA). To further analysis protein involvement, we have performed western blotting methodology.

2.4. Bioinformatic tools

E-GEOD-61351 and E-GEOD-57764, both available at ArrayExpress, were chosen for this analysis. E-GEOD-61351 dataset, which is based on GPL13112 platform (Illumina HiSeq 2000 [Mus musculus]), contains 6 IDG-SW3 samples differentiated for 28 days, treated (n = 3) or not (n = 3) with PTH. E-GEOD-57764 dataset, based on Agilent-G4851A SurePrint G3 Human GE 8 × 60K Microarray, which contains samples from human primary airway smooth muscle cultured for 24 h in three conditions, Control (n = 4), FCS (n = 4) and FCS + Dex (n = 4). The processed data were downloaded, and GEO2R [https://www.ncbi.nlm.nih.gov/geo/geo2r/] was used to calculate the differential expression of targets. P value < 0.01 and $|\log2FC| > 2$ was considered as differentially expressed. R was used to draw heatmap graphs with the base package, and TCGAbiolinks package was used to draw a Volcano plot.

2.5. Statistical analysis

All experiments were performed in triplicate (independent replicates) and the data expressed as the mean ± standard deviation (SD). They were verified using One-Way ANOVA with Tukey's post-test to compare all pairs of groups (where $p < 0.05$ was considered statistically significant; $p < 0.0001$ highly significant). The software used was GraphPad Prism 6. ImageJ Software was used for vesicles and osteocytes counting. For the statistical analysis, qPCR data were standardized considering fold changes of the control.

3. Results

3.1. Endothelial cells and smooth muscle cells contribute to the osteogenic phenotype

Human coronary aorta endothelial cells (a_EC) and aortic smooth muscle cells (VSMCs) significantly stimulated osteogenesis, as indicated by the upregulation of transforming growth factor beta 1 (TGFB1) (Fig. 1a), bone morphogenetic protein 2 (BMP2) (Fig. 1e), and growth differentiation factor 2 (GDF2) mRNA (Fig. 1f). Additionally, bone morphogenetic protein receptor type 1B (BMPR1B) (Fig. 1b) was upregulated. Both RUNX family transcription factor 2 (RUNX2) (Fig. 1g) and ALPL mRNA (Fig. 1i) were upregulated in response to a_EC and VSMCs, while osterix (SP7) mRNA was significantly upregulated specifically in response to VSMCs (Fig. 1h). The involvement of TGFB1/BMP signaling was validated by the upregulation of SMAD family members 2, 3, 4, 6, and SMAD7 mRNA (Figs. S2a–f).

Interestingly, vein-obtained endothelial cells (v_EC) delivered a pool of molecules with low osteogenic stimulus, as none of the evaluated biomarkers responded to v_EC-conditioned medium. This finding prompted further investigation into the role of VSMCs, which showed a pronounced effect on the osteogenic phenotype of osteoblasts. VSMCs upregulated the expression of TGFB1, osterix, and RUNX2 (Fig. 1), as well as SMADs. Importantly, VSMCs demonstrated greater effectiveness in promoting the osteogenic phenotype compared to endothelial cells.

3.2. VSMCs, not endothelial cells, promote osteoblast-to-osteocyte transition

Unexpectedly, the morphology of osteoblasts responding to trophic factors released by VSMCs was very similar to that of osteocytes (Fig. 2a). The number of in-vitro-differentiated cells was significantly greater in response to VSMCs compared to endothelial cells (Fig. 2b).

Table 1
Expression primers sequences and PCR cycle conditions. NCBI ID for gene and miRbase accession for the miRNAs.

Gene (ID)	Primer	5′-3′ Sequence	Reaction' Condition
BMPR2 (659)	Forward	CATATTAGGCGTGTGCCAAAAA	95 °C - 3s; 60 °C - 8s; 72 °C - 20s
	Reverse	GCTTGTGCTTGCTGTCGTTC	
BMPR1B (658)	Forward	ATTTGCAGCACAGACGGATATT	95 °C - 3s; 60 °C - 8s; 72 °C - 20s
	Reverse	GACACTGAAAATCTGAGCCTTCT	
BMP2 (650)	Forward	CCCAGCGTGAAAGAGGAGAC	95 °C - 3s; 60 °C–8 s; 72 °C - 20 s
	Reverse	CCATGGTCGACCTTTAGGAG	
BMP7 (655)	Forward	ACTGTGAGGGGGAGTGTGC	95 °C - 3s; 60 °C - 8s; 72 °C - 20 s
	Reverse	CGAAGTAGAGGACGGAGATGG	
SMAD2 (4087)	Forward	GCCGCCAGTTGTGAAGAGAC	95 °C - 3s; 60 °C–8 s; 72 °C - 20 s
	Reverse	TGGAGACGACCATCAAGAGACC	
SMAD3 (4088)	Forward	GCTGACACGGAGACACATCG	95 °C - 3 s; 60 °C–8 s; 72 °C–20 s
	Reverse	AGCCTCAAAGCCCTGGTTG	
SMAD4 (4089)	Forward	CTTTGAGGGACAGCCATCGT	95 °C - 3 s; 60 °C–8 s; 72 °C - 20s
	Reverse	GCCACAGAAATGTTGGGAAA	
SMAD5 (4090)	Forward	GTAAAACGACGGCCAGTTTTCATGGTGAATACTAAGACTGGTTT	95 °C - 3 s; 60 °C - 8 s; 72 °C - 20 s
	Reverse	TTCAATGTAAGCTCACAGTATCTGTACTC	
SMAD6 (4091)	Forward	TACTCTCGGCTGTCTCCTC	95 °C - 3 s; 60 °C - 8 s; 72 °C - 20 s
	Reverse	GAGTTGGTAGCCTCCGTTTC	
SMAD7 (4092)	Forward	GCTGAAACAGGGGGAACGA	95 °C - 3s; 60 °C - 8s; 72 °C - 20s
	Reverse	AGTATGCCACCACGCACCA	
TGFB1 (7040)	Forward	CAACGAAATCTATGACAAGTTCAAGCAG	95 °C - 3 s; 60 °C - 8 s; 72 °C - 20 s
	Reverse	CTTCTCGGAGCTCTGATGTG	
RUNX2 (860)	Forward	CCGTCCATCCACTCTACCAC	95 °C - 3 s; 60 °C - 8 s; 72 °C - 20 s
	Reverse	ATGAAATGCTTGGGAACTGC	
SP7 (121340)	Forward	CCAGGCAACACTCCTACTCC	95 °C - 3 s; 60 °C - 8 s; 72 °C - 20 s
	Reverse	GCCTTGCCATACACCTTGC	
TNFSF11 (8600)	Forward	AGGGACTCCATCCAAGAAGG	95 °C - 3 s; 60 °C - 8 s; 72 °C - 20 s
	Reverse	GCAGTTTCTGTTCTATTATTCAGGTG	
SOST (50964)	Forward	GCGTTCAAGAATGATGCCACG	95 °C - 3 s; 60 °C - 8 s; 72 °C - 20 s
	Reverse	GCTGTACTCGGACACGTCTTTGG	
DMP1 (1758)	Forward	CAGTGAGGATGAGGCAGACA	95 °C - 3 s; 60 °C - 8 s; 72 °C - 20 s
	Reverse	TCGATCGCTCCTGGTACTCT	
FGF23 (8074)	Forward	TGAGCGTCCTCAGAGCCTAT	95 °C - 3 s; 60 °C - 8 s; 72 °C - 20 s
	Reverse	TTGTGGATCTGCAGGTGGTA	
FGFR1 (2260)	Forward	CTGGGTAGCAACGTGGAGTT	95 °C - 3 s; 60 °C - 8 s; 72 °C - 20 s
	Reverse	ACCATGCAGGAGATGAGGAA	
FGFR2 (2263)	Forward	GGAAAAGAACGGCAGTAAAT	95 °C - 3 s; 60 °C - 8 s; 72 °C - 20 s
	Reverse	GTAGTCTGGGGAAGCTGTAAA	
FGFR3 (2261)	Forward	GGGCTTCTTCCTGTTCATCC	95 °C - 3 s; 60 °C - 8 s; 72 °C - 20 s
	Reverse	AGGGACACCTGTCGCTTGA	
FGFR4 (2264)	Forward	AGATGCTCAAAGACAACGCCT	95 °C - 3 s; 60 °C - 8 s; 72 °C - 20 s
	Reverse	CGCACTTCCACGATCACGTA	
PTCH1 (5727)	Forward	GGGTCCTCGCTTACAAACTC	95 °C - 3 s; 60 °C - 8 s; 72 °C - 20 s
	Reverse	ATGATGCCATCTGCGTCTAC	
SUFU (51684)	Forward	GAGGGCGAAGTAATTTGTGG	95 °C - 3 s; 60 °C - 8 s; 72 °C - 20 s
	Reverse	AGCCCTCCTTCTGAGTGCTT	
SHH (6469)	Forward	CACCGAGCAGTGGATATGTG	95 °C - 3 s; 60 °C - 8 s; 72 °C - 20 s
	Reverse	AGTGGCCAGGAGTGAAACTG	
miR-23a (MI0000079)	Forward	CCGGCTGGGGTTCCTG	95 °C - 3 s; 60 °C - 8 s; 72 °C - 20 s
	Reverse	GGTCGGTTGGAAATCCCTGGC	
miR-17 (MI0000071)	Forward	TCAGAATAATGTCAAAGTGCTTACAGTGCAGG	95 °C - 3 s; 60 °C - 8 s; 72 °C - 20 s
	Reverse	GTCACCATAATGCTACAAGTGCCTTCACTC	
LRP5 (4041)	Forward	AAGGGTGCTGTGTACTGGAC	95 °C - 3 s; 60 °C - 8 s; 72 °C - 20 s
	Reverse	AGAAGAGAACTTACGGGAC	
CTNNB1 (1499)	Forward	GCGTGGACAATGGCTACTCAAG	95 °C - 3 s; 60 °C - 8 s; 72 °C - 20 s
	Reverse	GTCATTGCATACTGCCCGTCAA	
GSK3B (2932)	Forward	GACTAAGGTCTTCCGACCCC	95 °C - 3 s; 60 °C - 8 s; 72 °C - 20 s
	Reverse	TTAGCATCTGACGCTGCTGT	
DKK1 (22943)	Forward	CCTTGGATGGGTATTCCAGA	95 °C - 3 s; 60 °C - 8 s; 72 °C - 20 s
	Reverse	CCTGAGGCACAGTCTGATGA	
SFRP1 (6422)	Forward	CGGCCAGCGAGTACGACTACGTGAGC	95 °C - 3 s; 60 °C - 8 s; 72 °C - 20 s
	Reverse	GCATCTCGGGCCAGATAGAAGCCGAAG	
SFRP2 (6423)	Forward	CTCGCTGCTGCTGCTCTTC	95 °C - 3 s; 60 °C - 8 s; 72 °C - 20 s
	Reverse	GGCTTCACATACCTTTGGAG	
CD9 (928)	Forward	TTTAAAAGTGCAGCCGGAGA	95 °C - 3 s; 60 °C - 8 s; 72 °C - 20 s
	Reverse	GCGCCGATGATGTGGAATTT	
CD63 (967)	Forward	TGATGCCGTGGAAAGCAGAT	95 °C - 3 s; 60 °C - 8 s; 72 °C - 20 s
	Reverse	AGTCAAGCGTCTCGTGGAAG	
CD81 (975)	Forward	GCGGTGGAAGGAGGAATGAA	95 °C - 3 s; 60 °C - 8 s; 72 °C - 20 s
	Reverse	AGCCCCCTGGATTATGGTCT	
AHSG (197)	Forward	GAATTCCCCGCTCATCCTGTTCT	95 °C - 3 s; 60 °C - 8 s; 72 °C - 20 s
	Reverse	CGTGGAAATCGCAGTCTCCT	
ALPL (249) TNAP	Forward	TTTATAAGGCGGCGGGGGTG	95 °C - 3 s; 60 °C - 8 s; 72 °C - 20 s
	Reverse	AGCCCAGAGATGCAATCGAC	

(*continued on next page*)

Table 1 (*continued*)

Gene (ID)	Primer	5′-3′ Sequence	Reaction' Condition
ENPP1 (5167)	Forward	TTTGCCGATTGAGGATTTTC	95 °C - 3 s; 60 °C - 8 s; 72 °C - 20 s
	Reverse	CCACTGACGACATTGACACC	
SMPD3 (55512)	Forward	GCCTATCACTGTTACCCCAAC	95 °C - 3 s; 60 °C - 8 s; 72 °C - 20 s
	Reverse	GACGATTCTTTGGTCCTGAGG	
PDPN (10630)	Forward	GGGAACGATGTGGAAGGTGT	95 °C - 3 s; 60 °C - 8 s; 72 °C - 20 s
	Reverse	GCTCTTTAGGGCGAGTACCT	
NOTCH1 (4851)	Forward	GGAAGTGTGAAGCGGCCAATG	95 °C - 3 s; 60 °C - 8 s; 72 °C - 20 s
	Reverse	ATAGTCTGCCACGCCTCTGC	
NOTCH2 (4853)	Forward	TGTCGAGATGGCTATGAACCCTG	95 °C - 3 s; 60 °C - 8 s; 72 °C - 20 s
	Reverse	GCAGCGGTTCTTCTCACAGG	
NOTCH3 (4854)	Forward	TGTCTGCCAGAGTTCAGTGGTG	95 °C - 3 s; 60 °C - 8 s; 72 °C - 20 s
	Reverse	AGGAGCAGAGGAAGCGTCCATC	
NOTCH4 (4855)	Forward	TTGTCCTCCCTCCTTCTGTTCC	95 °C - 3 s; 60 °C - 8 s; 72 °C - 20 s
	Reverse	AGAAGTCCCGAAGCTGGCAC	
JAG1 (182)	Forward	TGCCTCTGTGAGACCAACTG	95 °C - 3 s; 60 °C - 8 s; 72 °C - 20 s
	Reverse	GTTGGGTCCTGAATACCCCT	
JAG2 (3714)	Forward	GTGGCAAGAACTGCTCCGTG	95 °C - 3 s; 60 °C - 8 s; 72 °C - 20 s
	Reverse	TGCCTCTGTGAGACCAACTG	
GDF2 (2658)	Forward	AGAACGTGAAGGTGGATTTCC	95 °C - 3 s; 60 °C - 8 s; 72 °C - 20 s
	Reverse	CGCACAATGTTGG ACGCTG	
ITGB1 (3688)	Forward	GCCGCGCGGAAAAGATGAA	95 °C - 3 s; 60 °C - 8 s; 72 °C - 20 s
	Reverse	TGCTGTTCCTTTGCTACGGT	
SRC (6714)	Forward	CAACACAGAGGGAGACTGGT	95 °C - 3 s; 60 °C - 8 s; 72 °C - 20 s
	Reverse	AGCTTCTTCATGACCTGGGC	
PTK2 (5747)	Forward	TCAGCTCAGCACAATCCTGG	95 °C - 3 s; 60 °C - 8 s; 72 °C - 20 s
	Reverse	CTGAAGCTTGACACCCTCGT	
CFL1 (1072)	Forward	TGTGCGGCTCCTACTAAACG	95 °C - 3 s; 60 °C - 8 s; 72 °C - 20 s
	Reverse	TCCTTGACCTCCTCGTAGCA	
AKT1 (207)	Forward	CAGCGCGGCCCGAAGGAC	95 °C - 3 s; 60 °C - 8 s; 72 °C - 20 s
	Reverse	GACGCTACAGCGCTCCTCTC	
MAPK3 (5595)	Forward	AACAGGCTCTGGCCCACCCAT	95 °C - 3 s; 60 °C - 8 s; 72 °C - 20 s
	Reverse	GCAGCGCCTCCCTTGCTAGA	
MAPK8 (5599)	Forward	AAAGGTGGTGTTTTGTTCCCAGGT	95 °C - 3 s; 60 °C - 8 s; 72 °C - 20 s
	Reverse	TGATGATGGATGCTGAGAGCCATTG	
MAPK14 (1432)	Forward	GAGAACTGCGGTTACTTA	95 °C - 3 s; 60 °C - 8 s; 72 °C - 20 s
	Reverse	ATGGGTCACCAGATACACAT	
ALPL (249)	Forward	CGGGCACCATGAAGGAAA	95 °C - 3 s; 60 °C - 8 s; 72 °C - 20 s
	Reverse	GGCCAGACCAAAGATAGAGTT	
IBSP (3381)	Forward	GTTGCGTCTTGGAAGTGAGA	95 °C - 3 s; 60 °C - 8 s; 72 °C - 20 s
	Reverse	CAGCTGGCTGATCACTCAAA	
SPP1 (6696)	Forward	AGCAAGAAGCCCTGCCTGA	95 °C - 3 s; 60 °C - 8 s; 72 °C - 20 s
	Reverse	TCCTACTTACACCTGGACAGGATT	
BGLAP (632)	Forward	ATGAGAGCCCTCACACTCCTC	95 °C - 3 s; 60 °C - 8 s; 72 °C - 20 s
	Reverse	GCCGTAGAAGCGCCGATAGGC	
MMP2 (4313)	Forward	AGCTCCCGGAAAAGATTGATG	95 °C - 3 s; 60 °C - 8 s; 72 °C - 20 s
	Reverse	CAGGGTGCTGGCTGAGTAGAT	
MMP9 (4318)	Forward	CACGCACGACGTCTTCCA	95 °C - 3 s; 60 °C - 8 s; 72 °C - 20 s
	Reverse	AAGCGGTCCTGGCAGAAAT	
TIMP1 (7076)	Forward	CCGCAGCGAGGAGTTTCTC	95 °C - 3 s; 60 °C - 8 s; 72 °C - 20 s
	Reverse	GAGCTAAGCTCAGGCTGTTCCA	
TIMP2 (7077)	Forward	CGACATTTATGGCAACCCTATCA	95 °C - 3 s; 60 °C - 8 s; 72 °C - 20 s
	Reverse	GGGCCGTGTAGATAAACTCTATATCC	
RECK (8434)	Forward	TGCAAGCAGGCATCTTCAAA	95 °C - 3 s; 60 °C - 8 s; 72 °C - 20 s
	Reverse	ACCGAGCCCATTTCATTTCTG	
COL1A1 (1277)	Forward	AACCAAGGCTGCAACCTGGA	95 °C - 3 s; 60 °C - 8 s; 72 °C - 20 s
	Reverse	GGCTGAGTAGGGTACACGCAGG	
WNT1 (7471)	Forward	CCTTGCGCTCCCTGGATAAA	95 °C - 3 s; 60 °C - 8 s; 72 °C - 20 s
	Reverse	TGTTGGGTTCATGGCAGGTT	
GAPDH (2597)	Forward	GACTCATGACCACAGTCCATGC	95 °C - 3 s; 60 °C - 8 s; 72 °C - 20 s
	Reverse	AGAGGCAGGGATGATGTTCTG	

Importantly, all markers known to identify the osteocyte phenotype were significantly upregulated in osteoblasts responding to VSMCs, including dentin matrix acidic phosphoprotein 1 (DMP1) (approximately 15-fold increase, Fig. 2c), sclerostin (SOST) (approximately 15-fold increase, Fig. 2d), fibroblast growth factor 23 (FGF23) (approximately 15-fold increase, Fig. 2f), and miR-23a (approximately 12-fold increase, Fig. 2e), while glycoprotein 38 (PDPN) was higher in response to v_ECs (Fig. 2g).

Additionally, the osteocyte-acquired phenotype in response to VSMCs was viable, as indicated by the significant upregulation of mitogen-activated protein kinase (MAPK) and AKT serine/threonine kinase (AKT1) related genes (Fig. S3). We hypothesized that the increase in osteocyte biomarkers in osteoblasts is facilitated by vesicular communication from VSMCs. Our investigation revealed that VSMCs express these genes, showing significant increases in DMP1 (Fig. S4a) and SOST mRNA (Fig. S4b), while v_ECs upregulated miR-23a (Fig. S4c) and FGF23 (Fig. S4d). This suggests that vesicles are involved in the paracrine signaling between VSMCs and osteoblasts. Finally, to further confirm the functionality of these osteocytes, we demonstrated the upregulation of the sonic hedgehog (SHH) signaling pathway and TNF superfamily member 11 (TNFSF11) (Figs. S5a–d), as well as genes of the fibroblast growth factor receptor (FGFR) family (Figs. S5e–h).

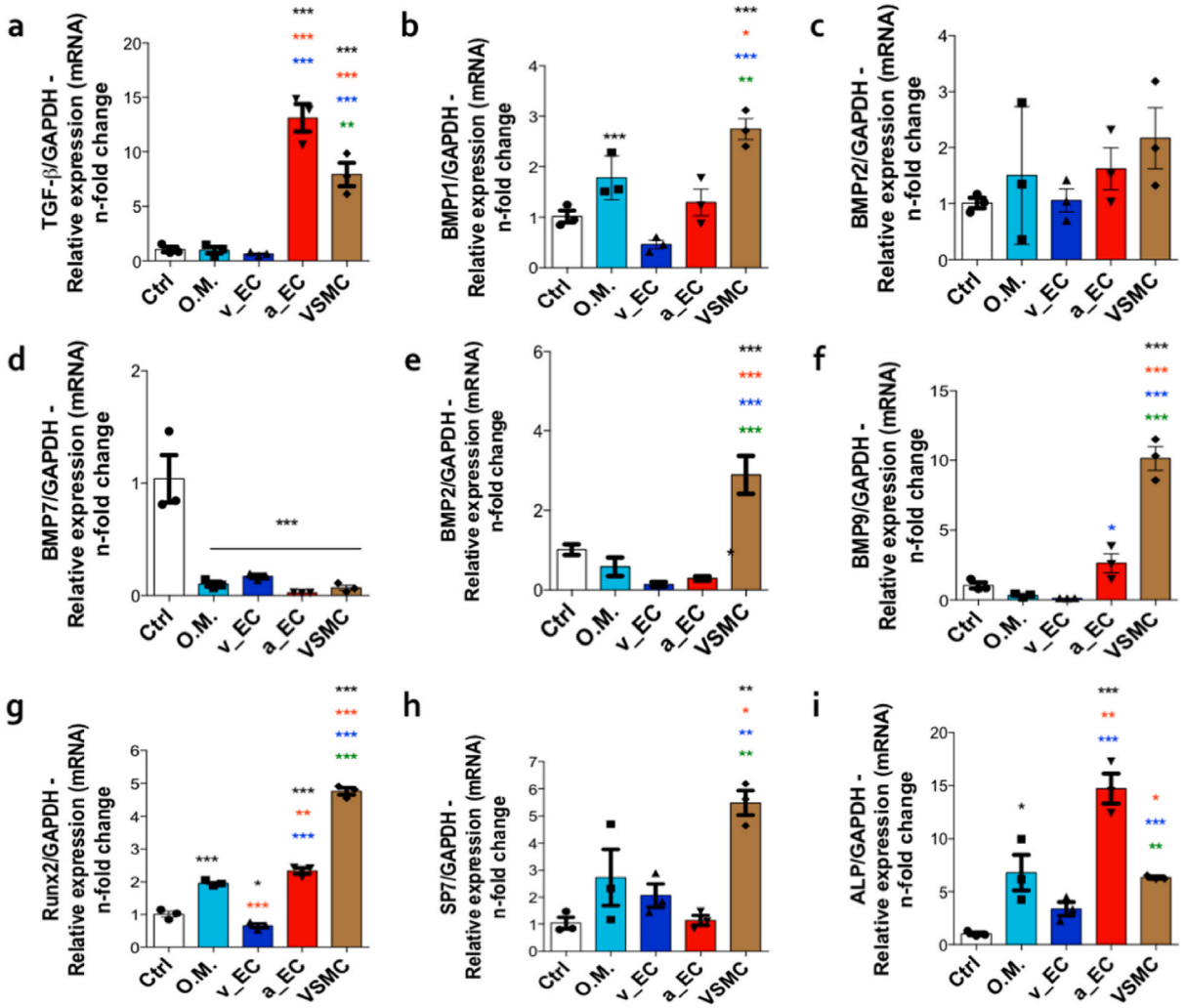

Fig. 1. Endothelial cells and VSMCs promote dynamic osteogenic gene marker reprogramming. After 28 days of treatment with the different conditioned media by primaries endothelial cells and VSMCs, osteoblasts were harvested in TRIzol. Thereafter, the mRNA was properly extracted to allow cDNA synthesis and further qPCR analysis. Firstly, the set of genes evaluated was: (**a**) TGFB1, (**b**) BMPR1B, (**c**) BMPR2, (**d**) BMP7, (**e**) BMP2, (**f**) GDF2, (**g**) SP7, (**h**) RUNX2, and (**i**) ALPL. The data were normalized using GAPDH expression (housekeeping gene). *$p < 0.05$; **$p < 0.1906$, ***$p < 0.0002$: Statistically significant difference when compared to control. *$p < 0.05$; **$p < 0.1906$; ***$p < 0.0002$: Statistical difference when compared with the Osteogenic medium. **$p < 0.1906$; ***$p < 0.0002$: Statistical difference when compared with the v_EC -conditioned medium. **$p < 0.1906$; ***$p < 0.0002$: Statistical difference when compared with the a_EC-conditioned medium.

3.3. VSMC releases exosomes containing osteocyte markers

We evaluated the capacity of endothelial and smooth muscle cells to express tetraspanins CD9, CD63, and CD81, which are biomarkers of exosomes [18] (Figs. S6–S9). Fig. 3 provides a comprehensive report on this matter, reinforcing their capacity to produce exosomes. Scanning electron microscopy clearly illustrated vesicles budding on the surface of both endothelial cells and VSMCs (Fig. 3a–f). Specifically, Fig. 3g shows the exosomes harvested from the conditioned medium of VSMCs, which were later subjected to nanoparticle tracking analysis (NTA) to verify vesicle size and amount (Fig. 3h).

We also investigated sphingomyelin phosphodiesterase 3 (SMPD3), an EV-related biogenesis gene, in endothelial cells and VSMCs (Fig. 3i). NTA analysis revealed a higher concentration of vesicles released by a_EC cells (5.31×10^8 exosomes/mL; Fig. 3j and k). Fig. 3l provides the zeta potential analysis, indicating that the exosomes obtained from VSMCs had the lowest value (<10 mV). This variation suggests the capacity of the exosomes to interact with the biophysical properties of the plasma membrane in target cells [22]. To conclude the exosome characterization, we investigated whether the exosomes could carry exosome-related tetraspanins (Fig. 3m–o) and SMPD3 transcripts (Fig. 3p).

After observing the effect of VSMCs on mature osteoblasts and demonstrating the relevance of exosomes in this communication, we decided to investigate whether these exosomes might be loaded with transcripts related to osteocyte gene markers. Surprisingly, our data indicated the presence of FGF23 transcripts (Fig. 4a; up to a 4-fold change), SOST (Fig. 4b; up to an 8-fold change), miR-23a (Fig. 4d; up to a 15-fold change), and PDPN (Fig. 4e; up to a 3-fold change). We also identified transcripts encoding catenin beta 1 (CTNNB1) signaling proteins loaded in the exosomes, such as secreted frizzled-related protein 1 (SFRP1), secreted frizzled-related protein 2 (SFRP2), dickkopf WNT signaling pathway inhibitor 1 (DKK1), and CTNNB1. Notably, DKK1 (Fig. 4h) and CTNNB1 (Fig. 4i) genes were upregulated in exosomes released by VSMCs.

3.4. VSMC promotes osteoblast-to-osteocyte transition by requiring β-catenin signaling

As discussed later, WNT/β-catenin signaling is critical in bone cells. We explored this signaling pathway during the osteoblast-to-osteocyte transition guided by vascular smooth muscle cells. Firstly, CTNNB1

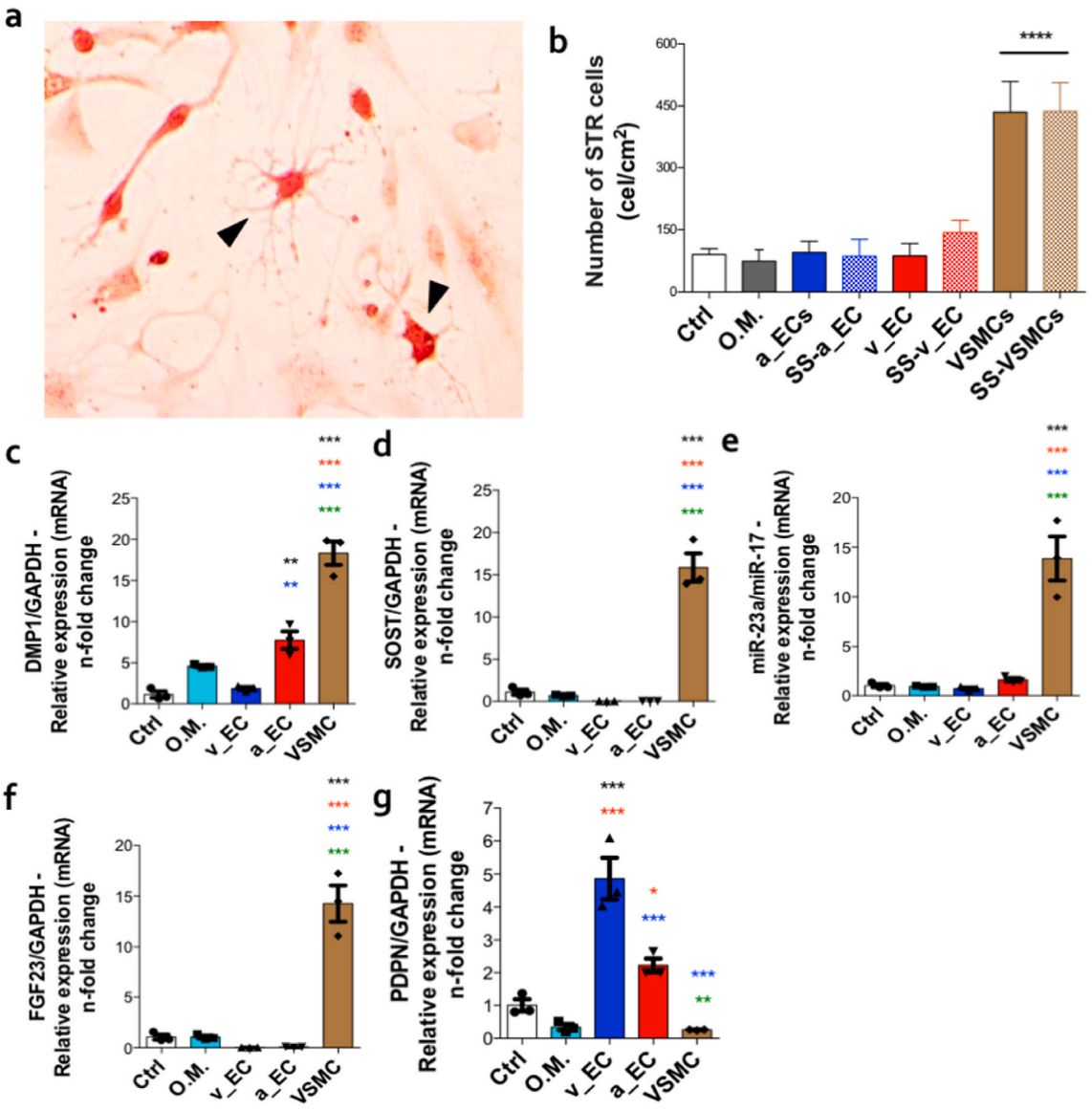

Fig. 2. VSMCs, but not endothelial cells, promotes osteoblast-to-osteocyte transition. Osteoblasts were challenged with the conditioned media obtained by the vascular cells (v_EC, a_EC, and VSMCs) up to 28 days, when the adherent cells were stained using Alizarin Red-S (**a**) and further differentiated osteocyte cells were quantified (**b**). Thereafter, the differentiated osteocytes were harvested to allow the analysis of osteocyte-related biomarkers by performing qPCR technology, as follows: (**c**) DMP1, (**d**) SOST, (**e**) miR-23a, (**f**) FGF23, and (**g**) PDPN. To note, the transcripts data were properly normalized with GAPDH, here considered a housekeeping gene, while miR-17 was used for normalizing the expression of miR-23a. **p < 0.1906; ***p < 0.0002, ****p < 0.0001: Statistically significant difference when compared to control. *p < 0.05; ***p < 0.0002: Statistical difference when compared with the osteogenic medium. **p < 0.1906; ***p < 0.0002: Statistical difference when compared with the v_EC -conditioned medium. **p < 0.1906; ***p < 0.0002: Statistical difference when compared with the a_EC-conditioned medium.

(Fig. 5a), SFRP1 (Fig. 5b), SFRP2 (Fig. 5c), and DKK1 (Fig. 5d) genes were evaluated in endothelial cells and VSMCs. Additionally, analysis of CTNNB1 at the protein level using laser confocal microscopy showed a significant distribution in VSMCs compared to endothelial cells (Fig. 5e).

We also demonstrated that exosomes released by VSMCs were loaded with both total and phosphorylated (S368) CTNNB1 (Fig. 5f and g). Our results clearly show that VSMCs release sufficient signals to promote osteoblast-to-osteocyte transition via CTNNB1, suggesting a regulatory role for these signals in this process. The involvement of the CTNNB1 signaling pathway in differentiated osteocytes in response to VSMCs was validated by quantitative RT-qPCR technology (Fig. 5h–n).

Additionally, differentiated osteocytes overexpressed transcripts of CTNNB1 (Fig. 5h), SFRP1 (Fig. 5i), SFRP2 (Fig. 5j), and DKK1 (Fig. 5k), as well as transcripts of Wnt family member 1 (WNT1) (Fig. 5l), LDL receptor-related protein 5 (LRP5) (Fig. 5m), and glycogen synthase kinase 3 beta (GSK3B) (Fig. 5n). Moreover, the importance of CTNNB1 in this scenario is further reinforced by the presence of WNT/β-catenin-related genes in the transcript pool of exosomes released by endothelial cells.

3.5. *Influence of endothelial and smooth muscle cells on osteocyte adhesion and mineralization*

We elucidated a strong influence of both endothelial and smooth muscle cells on osteocyte adhesion by modulating the expression of integrin subunit beta 1 (ITGB1), SRC proto-oncogene, non-receptor tyrosine kinase (SRC), protein tyrosine kinase 2 (PTK2), and cofilin (CFL1), a protein related to cytoskeleton rearrangement necessary during the osteoblast-to-osteocyte transition. Part of our results was validated using global transcriptome data obtained from ArrayExpress (E-

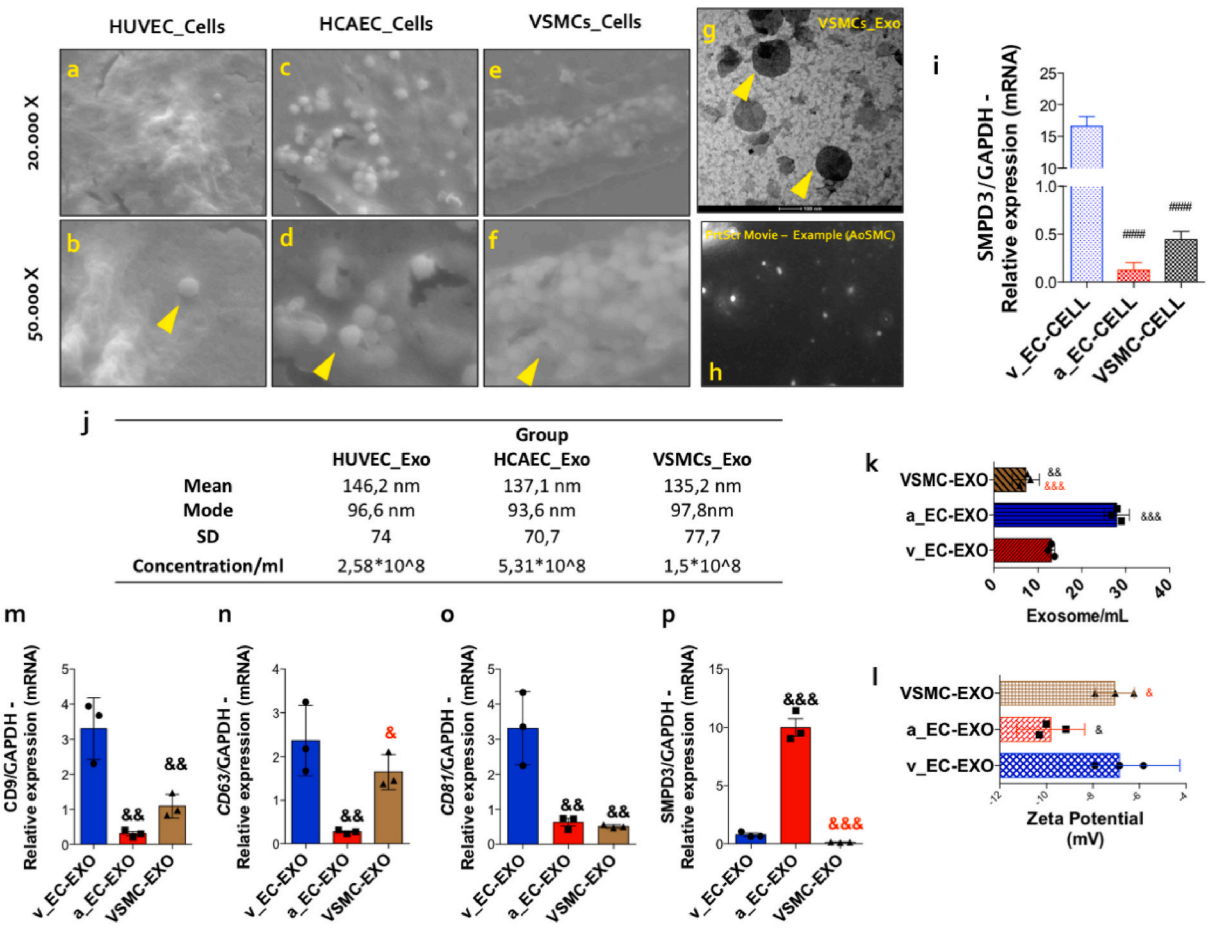

j

	Group		
	HUVEC_Exo	HCAEC_Exo	VSMCs_Exo
Mean	146,2 nm	137,1 nm	135,2 nm
Mode	96,6 nm	93,6 nm	97,8nm
SD	74	70,7	77,7
Concentration/ml	2,58*10^8	5,31*10^8	1,5*10^8

Fig. 3. Characterization of EVs released by endothelial cells and VSMCs. Cultures of vascular cells (v_EC, a_EC, and VSMCs) were maintained up to 72 h, when their specific conditioned media was collected to further evaluate whether exosomes were released. Firstly, the cells were properly prepared to be analyzed in electron microscopy and extracellular vesicles were observed interacting with the plasma membrane of those cells (**a-f**). After collecting the medium, the EVs were pooled as detailed in material and methods, and duly characterized as recommended in MISEV2018. Secondly, the EVs were analyzed in transmission electron microscopy (g) and the EVs dispersion was noticed. The vascular cells were evaluated regarding their capacity in expressing SMPD3 gene, a marker of biogenesis of EVs in eukaryotic cells (**i**). Additionally, the EVs size and concentration was performed by nanoparticles tracking analysis (NTA) (**h**, **j–k**). Thereafter, EVs were evaluated considering their zeta potential (**l**). Lastly, the EVs cargo was evaluated in relation to their capacity to carry tetraspanin transcripts, such as (**m**) CD9, (**n**) CD63, and (**o**) CD81, as well as transcripts of SMPD3 (**p**). ####p < 0.0001: Statistical difference when compared with the v_EC cells. &p < 0.05; &&p < 0.1906; &&&p < 0.0002: Statistical difference when compared with the v_EC exosome. &p < 0.05; &&p < 0.1906. Statistical difference when compared with the a_EC exosome.

GEOD-61351; Fig. S10). Additionally, Notch signaling-related members were also upregulated in osteocytes obtained in response to VSMCs (Fig. S11).

We suggest that these experimentally obtained osteocytes are functional cells, as indicated by the increase in extracellular matrix (ECM) remodeling-related genes encoding collagen type I alpha 1 chain (COL1A1) (Fig. S12a), matrix metallopeptidase 2 (MMP2) (Fig. S12b), and matrix metallopeptidase 9 (MMP9) (Fig. S12c). VSMCs also stimulated the upregulation of MMP-related tissue inhibitors, such as TIMP metallopeptidase inhibitor 1 (TIMP1), TIMP metallopeptidase inhibitor 2 (TIMP2), and reversion-inducing cysteine-rich protein with kazal motifs (RECK), indicating that these mechanisms are decisive in osteocytes, potentially for maintaining pericellular remodeling (Figs. S12d–f).

Finally, we investigated mechanisms related to the mineralizing phenotype of osteocyte biology (Fig. 6a). First, we demonstrated the capacity of exosomes released by endothelial and smooth muscle cells to deliver ATP (Fig. 6b). Among them, a_EC and VSMCs significantly increased their ATP content in response to the mechanotransduction process (Fig. 6b). Genes related to the mineralizing process, such as ectonucleotide pyrophosphatase/phosphodiesterase 1 (ENPP1), alkaline phosphatase, biomineralization associated (TNAP), and alpha 2-HS glycoprotein (AHSG), were also investigated (Fig. 6f–h; extended results in Fig. S13). Together, our results confirm the strong influence of blood vessels in promoting the mineralizing phenotype of terminally differentiated osteocytes.

4. Discussion

We have tested the hypothesis that VSMCs (vascular smooth muscle cells) affect osteoblast differentiation and their capacity to differentiate into osteocytes through exosome communication. Our data demonstrate a very active crosstalk between VSMCs and osteoblasts, reinforcing the already known relevance of blood vessels in coordinating osteoblasts and osteoclasts during bone remodeling [23–27]. Additionally, this study is the first to show a novel mechanism by which VSMCs drive osteoblast-to-osteocyte transition by releasing exosomes to deliver morphogenetic signals.

In addition to their well-known roles in blood circulation, researchers increasingly seek to understand how vascular cells contribute to bone homeostasis and the physiological mechanisms maintaining skeletal health. Although significant progress has been made [10,12, 28–35], yet information remains scarce about the circulating molecules that drive bone cell phenotypes. Studies on the crosstalk between vasculature and bone cells are supported by the fact that bone is highly

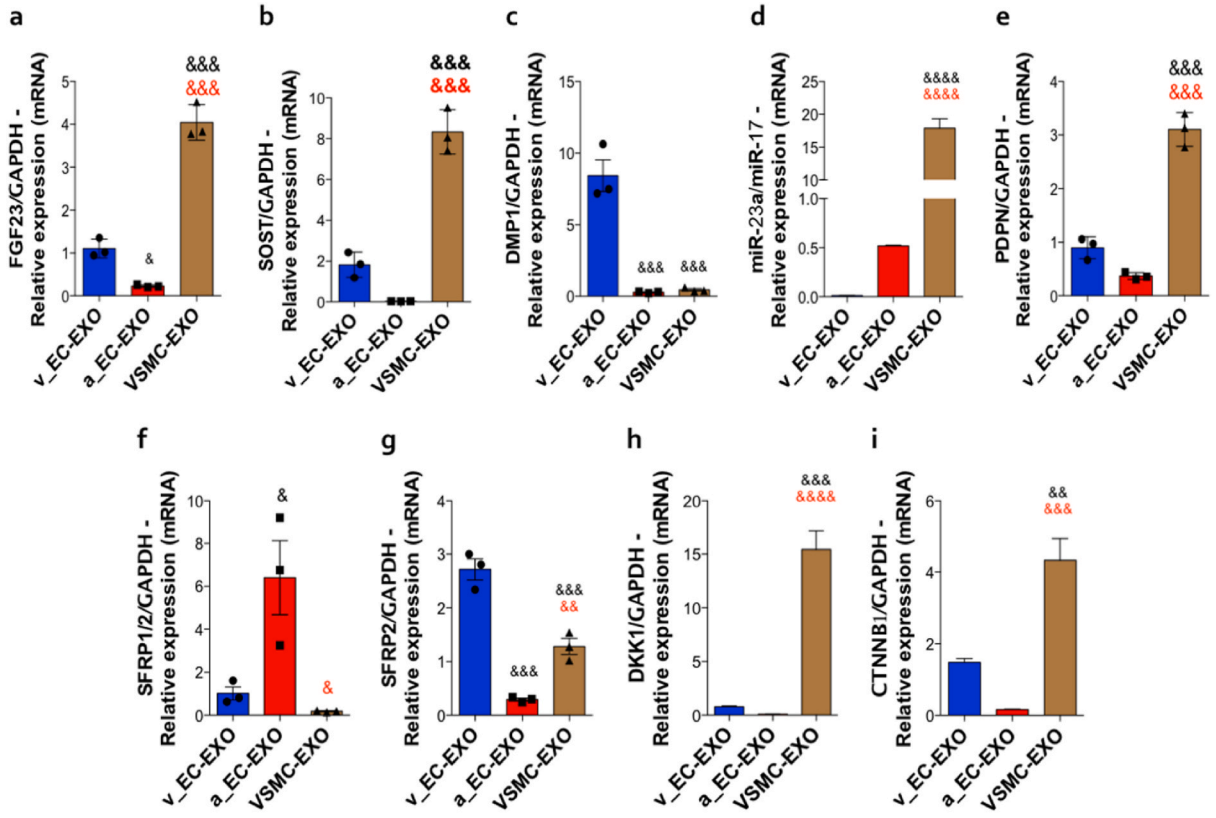

Fig. 4. Exosomes cargo released by vascular cells reveals a source of osteocyte related biomarkers and β**-catenin signaling members.** Briefly, the exosomes were properly isolated, and total mRNA pooled to allow the synthesis of cDNA and further applied in qPCR machine. The transcripts analyzed were as follows: FGF23 (**a**), SOST (**b**), DMP1 (**c**), miR-23a (**d**), and Gp38 (**e**). Importantly, transcripts of the β-catenin signaling pathway were also investigated in Exosome cargo and the analysis reveals those vesicles carrying SFRP1 (**f**), SFRP2 (**g**), DKK1 (**h**), β-catenin (**i**). GAPDH transcripts was used as housekeeping gene, and miR-17 transcripts used to normalize the expression of miR-23a. &p < 0.05; &&&p < 0.0002; &&&&p < 0.0001: Statistical difference when compared with the v_EC exosome. &p < 0.05; &&&p < 0.0002; &&&&p < 0.0001: Statistical difference when compared with the a_EC exosome.

vascularized [36], and blood vessels are found in most regions of the skeletal system, except for growth plates and articular cartilage, maybe highlighting the relevance of hypoxia in coordinating the morphogenetic signals during bone development [37]. Indeed, bone formation and fracture healing are controlled by blood vessels [38].

While the coupling of bone cells and endothelial cells is clear, limited evidence supports the relevance of vascular smooth muscle cells in these processes. To evaluate the effect of endothelial and vascular smooth muscle cells on mature osteoblasts, medium conditioned by VSMCs was collected and further used to challenge human primary mature osteoblasts. Although alternative experimental approaches to minimize the use of animals have become widespread, in vitro studies also face limitations, such as the availability of primary human cells. Therefore, we explored primary human coronary aorta endothelial cells and aortic smooth muscle cells, which both significantly stimulated osteogenesis in vitro. This stimulation likely involves both local paracrine effects between cell types within bone and potential endocrine effects in vivo.

Mature osteoblasts responding to VSMC signals displayed the morphology and molecular machinery of terminally differentiated osteocytes. We confirmed this by evaluating SOST and DMP1 expression, both of which are well-accepting osteocyte markers. Moreover, miR-23a was identified in osteocytes obtained from these experiments, indicating its inclusion as a biomarker. Osteoblast-specific miR-23a cluster gain-of-function mice have low bone mass associated with decreased osteoblast but increased osteocyte numbers [39], which certainly impact bone mass by stimulating osteoclastogenesis. FGF23, part of a hormonal bone-parathyroid-kidney axis, is also synthesized and secreted by osteocytes and regulated by 1,25(OH)2D and serum phosphorus, among other factors [40].

To understand the differential stimuli exerted by endothelial cells, we investigated their effects on osteoblasts. Despite technical limitations focusing on phenotypic changes in osteoblasts using in vitro approaches, our study suggests synchrony between endothelial and vascular smooth muscle cells in promoting osteogenesis and bone remodeling. It seems endothelial cells stimulate genes necessary for maintaining the osteogenic phenotype, such as TGFB1 family members, corroborating findings on the influence of endothelial signaling on osteogenesis and bone deposition, while VSMCs provide sufficient signaling to drive mature osteoblasts toward osteocyte differentiation. Zeng et al. [2017] demonstrated that the miR-23a cluster regulates osteocyte differentiation by modulating the TGFB1 signaling pathway through targeting Prdm16, reinforcing the relevance of this mechanism orchestrated by endothelial cells as a prerequisite to osteocytogenesis promoted by VSMCs.

Briefly, our study provides novel findings into the role of VSMCs in releasing exosomes that drive osteocytogenesis. Osteocytes, the primary source of TNFSF11 in the body, are major contributors to bone resorption by signaling osteoclastogenesis [41–43]. Additionally, osteocytes connect with other bone cells, such as osteoblasts, monocytes, macrophages, and osteoclasts, through cytoplasmic processes passing through bone canaliculi [44,45]. Our findings show that this osteocytogenic effect is mediated by exosomes with a median diameter of approximately 120 nm, extending recent observations of the role of exosomes in bone biology [46]. Our data shows that VSMCs-released exosomes are loaded with regulatory molecules that orchestrate osteoblast-to-osteocyte transition via β-catenin, a crucial component of canonical WNT signaling. This finding aligns with evidence showing the WNT pathway is vital and evolutionarily conserved role in regulating differentiation

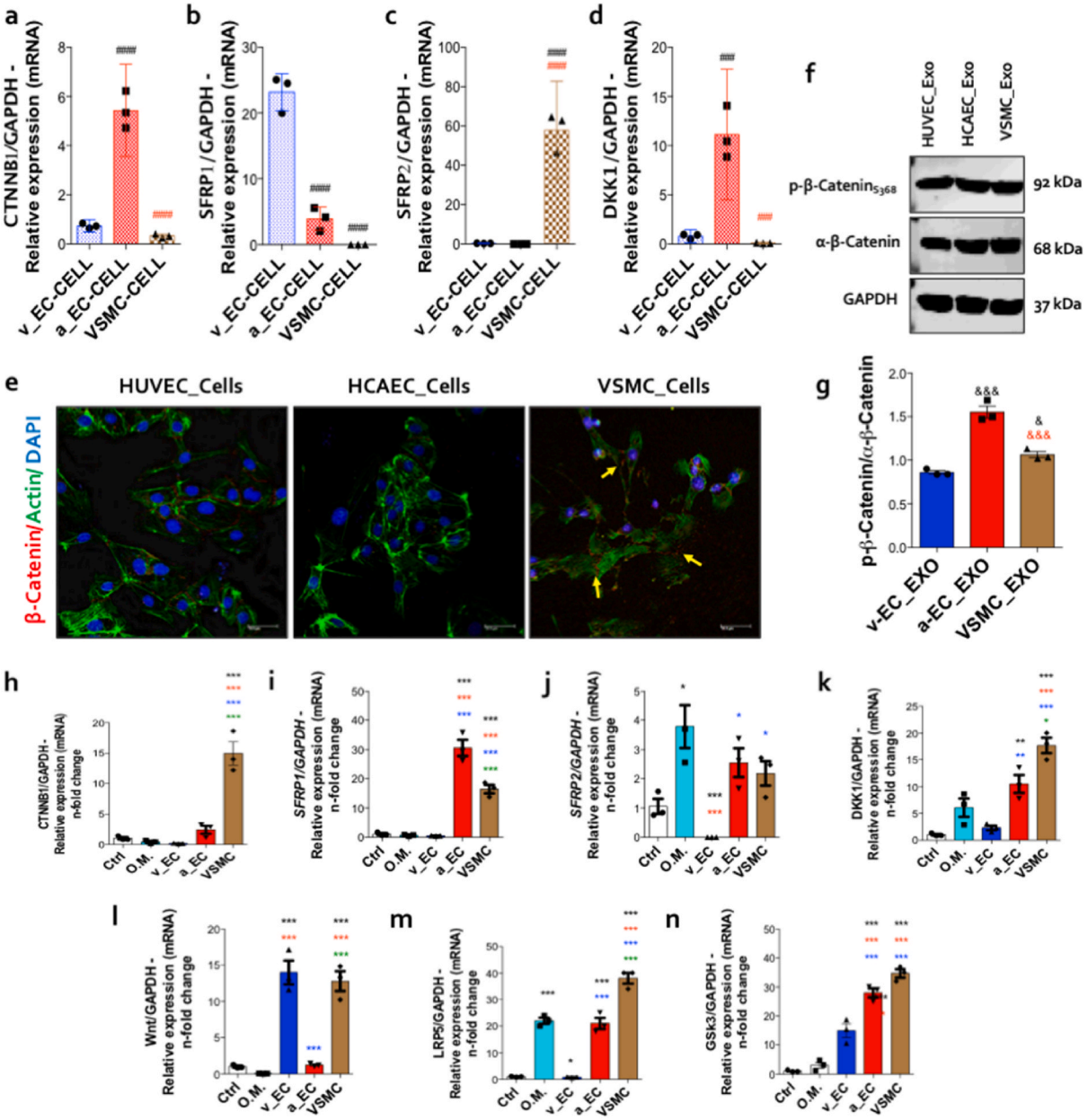

Fig. 5. Circumstantial WNT/β-catenin involvement in exosomes-induced osteoblast-to-osteocyte transition. CTNNB1 signaling was firstly evaluated in v_EC, a_EC, and VSMCs, considering CTNNB1(**a**), SFRP1 (**b**), SFRP2 (**c**), DKK1 (**d**), and in addition CTNNB1at protein level was detected in VSMCsusing laser confocal microscopy (**e**). Thereafter, both CTNNB1and phospho- CTNNB1(S368) was detected in exosomes released by vascular cells (**f,g**). Lastly, differentiated osteocytes were harvested in TRIzol to allow the analysis of transcripts related with CTNNB1signaling, such as: CTNNB1 (**h**), SFRP1 (**i**), SFRP2 (**j**), DKK1 (**k**), WNT1 (**l**), LRP5 (**m**), GSK3B (**n**). The data were normalized by GAPDH gene (housekeeping gene). ###p < 0.0002; ####p < 0.0001: Statistical difference when compared with the v_EC cells. ###p < 0.0002; ####p < 0.0001: Statistical difference when compared with the a_EC cells. &p < 0.05; &&&p < 0.0002: Statistical difference when compared with the v_EC exosome. &&&p < 0.0002: Statistical difference when compared with the a_EC exosome. *p < 0.05; **p < 0.1906; ***p < 0.0002: Statistically significant difference when compared to control. **p < 0.1906; ***p < 0.0002: Statistical difference when compared with the osteogenic medium. *p < 0.05; **p < 0.1906; ***p < 0.0002: Statistical difference when compared with the v_EC -conditioned medium. *p < 0.05; ***p < 0.0002: Statistical difference when compared with the a_EC-conditioned medium.

and organogenesis [47]. Our study highlights the complexity of this pathway, emphasizing the involvement of receptors (LRP4, 5, and 6), activators (WNTs), and inhibitors (SOST, DKK1, and SFRPs) in differentiated osteocytes' response to VSMCs [48–52].

Taking osteocyte biology into account, CTNNB1 is essential for maintaining cell viability, communication between osteocytes, bone integrity, response to anabolic loading, and mechanotransduction [53–57]. The relationship between blood flow and bone loss/formation, associated with conditions like osteoporosis and osteopetrosis, further underscores this complexity. Aging is linked to both bone loss and reduced skeletal blood flow, with Notch pathway genes implicated in these processes [29]. Summarizing, our findings clearly indicate that VSMC-released exosomes are sufficient to promote osteoblast-to-osteocyte transition through CTNNB1 signaling. This novel mechanism highlights the importance of vascular smooth muscle cells in bone remodeling, providing new insights into the intricate communication between bone cells and blood vessels. The active crosstalk between VSMCs and osteoblasts, mediated by exosomes, underscores the role of blood vessels in coordinating osteoblast and osteoclast activity, essential for maintaining bone homeostasis (Fig. 7).

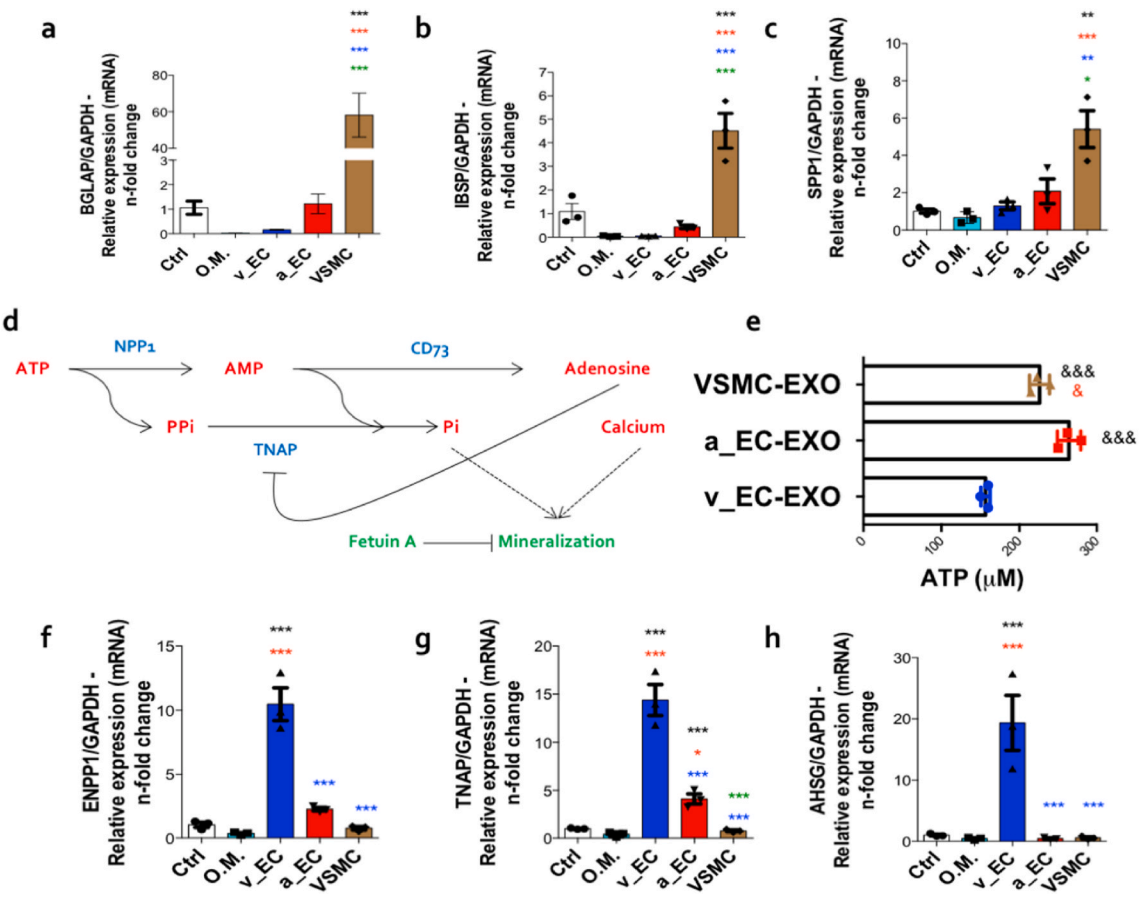

Fig. 6. Exosomes deliver ATP and modulate the transcription of genes related to bone mineralization. Differentiated osteocytes were evaluated focusing on mineralizing phenotype, and osteocalcin (BGLAP) (**a**), bone sialoprotein (IBSP) (**b**), and osteopontin (SPP1) (**c**) transcripts were significantly up-regulated in response to VSMCs. The schematization depicted in (**d**) suggests the involvement of ENPP1, TNAP, and AHSG, as well as ATP, in the mineralization mechanism. This lead to investigate them during the mechanism suggested in this study during osteoblast-to-osteocyte transition. ATP content was significantly higher in exosome cargo released by a_EC and VSMCs(**e**). Lastly, ENPP1 (**f**), TNAP (**g**), and AHSG (**h**) genes were evaluated in differentiated osteocytes. The data were normalized using GAPDH as housekeeping gene. &$p < 0.05$: Statistical difference when compared with the v_EC exosome. &&&$p < 0.0002$: Statistical difference when compared with the a_EC exosome. **$p < 0.1906$; ***$p < 0.0002$: Statistically significant difference when compared to control. *$p < 0.05$; ***$p < 0.0002$: Statistical difference when compared with the osteogenic medium. **$p < 0.1906$; ***$p < 0.0002$: Statistical difference when compared with the v_EC -conditioned medium; *$p < 0.05$; **$p < 0.1906$: Statistical difference when compared with the a_EC-conditioned medium.

The identification of key osteocyte markers and signaling pathways involved in this transition, such as SOST, DMP1, and miR-23a, further supports the significance of our findings. Additionally, the involvement of WNT/β-catenin signaling and other regulatory molecules in VSMC-derived exosomes suggests a complex regulatory network that drives osteocytogenesis. Despite these advances, our study also highlights several limitations, primarily the reliance on gene expression data to confirm cell phenotypes. Future research should focus on validating these findings by evaluating at protein level and functional levels to provide a more comprehensive understanding of the mechanisms involved. Specifically, studies should investigate the protein expression of key molecules, the functional outcomes of osteocyte differentiation, and the effects of inhibiting exosome secretion or CTNNB1 signaling. Furthermore, exploring the role of other signaling pathways and the interaction between endothelial cells and VSMCs in promoting osteogenesis and bone remodeling will be crucial. Understanding the endocrine effects of vascular cell-derived signals on bone health and disease could lead to the development of novel therapeutic strategies for bone-related disorders such as osteoporosis and osteogenesis imperfecta.

Finally, our study opens new avenues for understanding the role of VSMCs in bone biology and underscores the potential of targeting exosome-mediated communication for therapeutic interventions in bone-related diseases.

5. Conclusion

Our study reveals a novel and crucial mechanism by which vascular smooth muscle cells (VSMCs) promote the transition of osteoblasts to osteocytes through the release of exosomes loaded with regulatory molecules. This discovery underscores the importance of VSMCs in bone remodeling and skeletal homeostasis. The identification of key osteocyte markers and the involvement of WNT/β-catenin and miR-23a signaling pathways highlight the complexity of communication between bone and vascular cells. In addition to offering new insights into the role of vascular cells in bone biology, our findings pave the way for developing innovative therapeutic strategies targeting exosome-mediated communication for treating bone diseases such as osteoporosis. Future research should focus on validating these findings at the protein and functional levels, further exploring the interactions between endothelial cells and VSMCs in promoting osteogenesis and bone remodeling, with the potential for significant advancements in skeletal health and clinical applications.

Funding

FAPESP: Fundação de Amparo à Pesquisa do Estado de São Paulo (2014/22689-3; 2016/01139-0; 2017/18349-0) and Conselho Nacional

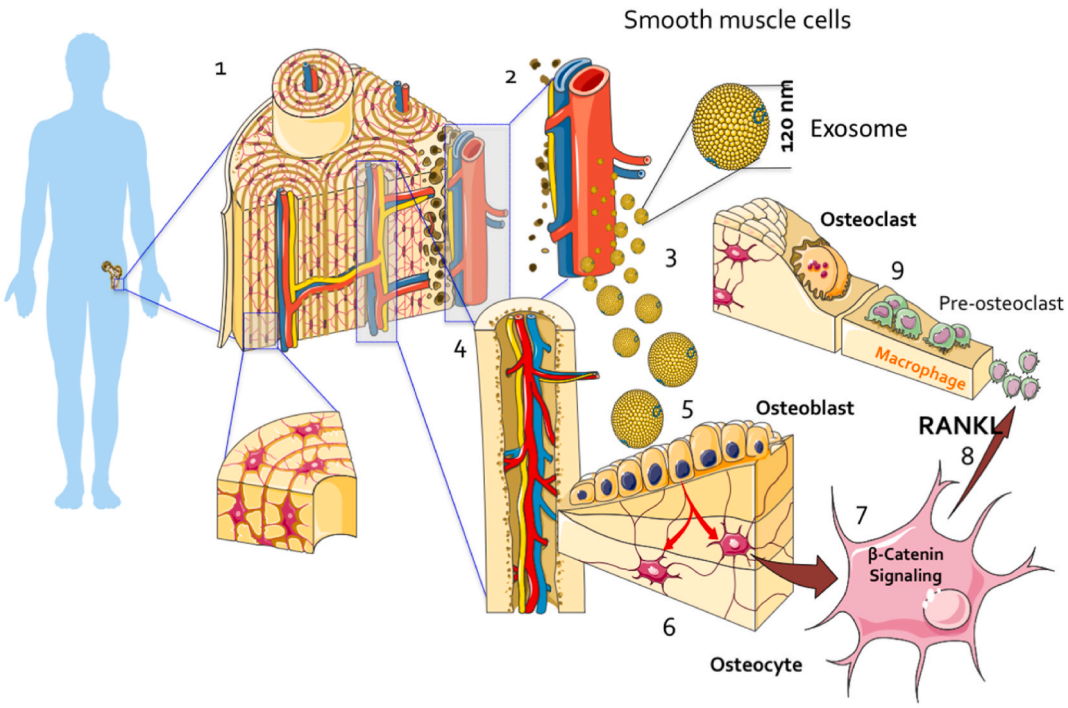

Fig. 7. Schematic representation of the main findings of this study. This schematization depicts an overview of the main data obtained in this study. Briefly, osteoblast cells obtained from healthy donors were grown in vitro (1) and challenged with conditioned medium by v_ECs, a_ECs, and VSMCs, separately. Altogether, the findings bring a new role of smooth muscle cells (2) in releasing exosomes (3) and driving osteoblast-to-osteocyte (4–6) transition via CTNNB1 signaling (7). As osteocytes are the major source of TNFSF11 (8), this proposed mechanism can contribute to osteoclastogenesis (9) and be related to bone-related disorders.

de Desenvolvimento Científico e Tecnológico (CNPq –314166/2021-1).

CRediT authorship contribution statement

Célio J.C. Fernandes: Writing – review & editing, Writing – original draft, Validation, Methodology, Investigation, Formal analysis, Conceptualization. **Rodrigo A. Silva:** Writing – review & editing, Writing – original draft, Methodology, Investigation, Formal analysis, Data curation. **Marcel R. Ferreira:** Writing – review & editing, Writing – original draft, Investigation, Formal analysis, Data curation, Conceptualization. **Gwenny M. Fuhler:** Writing – review & editing, Writing – original draft, Visualization, Software, Project administration, Formal analysis. **Maikel P. Peppelenbosch:** Writing – review & editing, Writing – original draft, Supervision, Resources, Project administration. **Bram CJ. van der Eerden:** Writing – review & editing, Writing – original draft, Visualization, Supervision, Project administration, Conceptualization. **Willian F. Zambuzzi:** Writing – review & editing, Writing – original draft, Visualization, Supervision, Resources, Project administration, Funding acquisition, Conceptualization.

Declaration of competing interest

The authors declare that they have no known competing financial interests or personal relationships that could have appeared to influence the work reported in this paper.

Data availability

Data will be made available on request.

Acknowledgments

The authors are grateful to Centro de Microscopia Eletrônica, IBB-UNESP, Botucatu-SP, for the confocal microscopy assistance.

Appendix A. Supplementary data

Supplementary data to this article can be found online at https://doi.org/10.1016/j.yexcr.2024.114211.

References

[1] K. Henriksen, A.V. Neutzsky-Wulff, L.F. Bonewald, M.A. Karsdal, Local communication on and within bone controls bone remodeling, Bone 44 (2009) 1026–1033.
[2] J. Klein-Nulend, P.J. Nijweide, E.H. Burger, Osteocyte and bone structure, Curr. Osteoporos. Rep. 1 (2003) 5–10.
[3] M.B. Schaffler, O.D. Kennedy, Osteocyte signaling in bone, Curr. Osteoporos. Rep. 10 (2012) 118–125.
[4] H.-C. Zeng, Y. Bae, B.C. Dawson, Y. Chen, T. Bertin, E. Munivez, P.M. Campeau, J. Tao, R. Chen, B.H. Lee, MicroRNA miR-23a cluster promotes osteocyte differentiation by regulating TGF-beta signalling in osteoblasts, Nat. Commun. 8 (2017) 15000.
[5] L.F. Bonewald, The amazing osteocyte, J. Bone Miner. Res. 26 (2011) 229–238.
[6] L.F. Bonewald, Mechanosensation and transduction in osteocytes, BoneKEy-Osteovision 3 (2006) 7–15.
[7] A.D. Bakker, K. Soejima, J. Klein-Nulend, E.H. Burger, The production of nitric oxide and prostaglandin E(2) by primary bone cells is shear stress dependent, J. Biomech. 34 (2001) 671–677.
[8] N. Yamamoto, T. Oyaizu, M. Enomoto, M. Horie, M. Yuasa, A. Okawa, K. Yagishita, VEGF and bFGF induction by nitric oxide is associated with hyperbaric oxygen-induced angiogenesis and muscle regeneration, Sci. Rep. 10 (2020) 2744.
[9] J.P. Cooke, D.W. Losordo, Nitric oxide and angiogenesis, Circulation 105 (2002) 2133–2135.
[10] S.K. Ramasamy, A.P. Kusumbe, L. Wang, R.H. Adams, Endothelial Notch activity promotes angiogenesis and osteogenesis in bone, Nature 507 (2014) 376–380.
[11] S.K. Ramasamy, A.P. Kusumbe, M. Schiller, D. Zeuschner, M.G. Bixel, C. Milia, J. Gamrekelashvili, A. Limbourg, A. Medvinsky, M.M. Santoro, et al., Blood flow controls bone vascular function and osteogenesis, Nat. Commun. 7 (2016) 13601.
[12] K.K. Sivaraj, R.H. Adams, Blood vessel formation and function in bone, Development 143 (2016) 2706–2715.
[13] A.M. Gomes, T.S. Pinto, C.J. da Costa Fernandes, R.A. da Silva, W.F. Zambuzzi, Wortmannin targeting phosphatidylinositol 3-kinase suppresses angiogenic factors in shear-stressed endothelial cells, J. Cell. Physiol. 235 (2020) 5256–5269.
[14] R.A. da Silva, M.R. Ferreira, A.M. Gomes, W.F. Zambuzzi, LncRNA HOTAIR is a novel endothelial mechanosensitive gene, J. Cell. Physiol. 235 (2020) 4631–4642.
[15] T.S. Pinto, CJ. da C. Fernandes, R.A. da Silva, A.M. Gomes, J.C.S. Vieira, P. de M. Padilha, W.F. Zambuzzi, c-Src kinase contributes on endothelial cells

mechanotransduction in a heat shock protein 70-dependent turnover manner, J. Cell. Physiol. 234 (2019) 11287–11303.
[16] R.A. da Silva, CJ. da C. Fernandes, G. da S. Feltran, A.M. Gomes, A.F. de Camargo Andrade, D.C. Andia, M.P. Peppelenbosch, W.F. Zambuzzi, Laminar shear stress-provoked cytoskeletal changes are mediated by epigenetic reprogramming of TIMP1 in human primary smooth muscle cells, J. Cell. Physiol. 234 (2019) 6382–6396.
[17] K.J. Livak, T.D. Schmittgen, Analysis of relative gene expression data using real-time quantitative PCR and the 2−ΔΔCT method, Methods 25 (2001) 402–408.
[18] C. Théry, K.W. Witwer, E. Aikawa, M.J. Alcaraz, J.D. Anderson, R. Andriantsitohaina, A. Antoniou, T. Arab, F. Archer, G.K. Atkin-Smith, et al., Minimal information for studies of extracellular vesicles 2018 (MISEV2018): a position statement of the International Society for Extracellular Vesicles and update of the MISEV2014 guidelines, J. Extracell. Vesicles 7 (2018) 1535750.
[19] P. Carpintero-Fernandez, J. Fafian-Labora, A. O'Loghlen, Technical advances to study extracellular vesicles, Front. Mol. Biosci. 4 (2017) 79.
[20] F. Momen-Heravi, L. Balaj, S. Alian, P.-Y. Mantel, A.E. Halleck, A.J. Trachtenberg, C.E. Soria, S. Oquin, C.M. Bonebreak, E. Saracoglu, et al., Current methods for the isolation of extracellular vesicles, Biol. Chem. 394 (2013) 1253–1262.
[21] A. Mehdiani, A. Maier, A. Pinto, M. Barth, P. Akhyari, A. Lichtenberg, An innovative method for exosome quantification and size measurement, J. Vis. Exp. 50974 (2015).
[22] E. Beit-Yannai, S. Tabak, W.D. Stamer, Physical exosome:exosome interactions, J. Cell Mol. Med. 22 (2018) 2001–2006.
[23] J. Chen, M. Hendriks, A. Chatzis, S.K. Ramasamy, A.P. Kusumbe, Bone vasculature and bone marrow vascular niches in health and disease, J. Bone Miner. Res. 35 (2020) 2103–2120.
[24] A.P. Kusumbe, S.K. Ramasamy, R.H. Adams, Coupling of angiogenesis and osteogenesis by a specific vessel subtype in bone, Nature 507 (2014) 323–328.
[25] A.P. Kusumbe, R.H. Adams, Osteoclast progenitors promote bone vascularization and osteogenesis, Nat Med 20 (2014) 1238–1240.
[26] S.K. Ramasamy, A.P. Kusumbe, R.H. Adams, Regulation of tissue morphogenesis by endothelial cell-derived signals, Trends Cell Biol. 25 (2015) 148–157.
[27] A.P. Kusumbe, S.K. Ramasamy, T. Itkin, M.A. Mäe, U.H. Langen, C. Betsholtz, T. Lapidot, R.H. Adams, Age-dependent modulation of vascular niches for haematopoietic stem cells, Nature 532 (2016) 380–384.
[28] U.H. Langen, M.E. Pitulescu, J.M. Kim, R. Enriquez-Gasca, K.K. Sivaraj, A. P. Kusumbe, A. Singh, J. Di Russo, M.G. Bixel, B. Zhou, et al., Cell-matrix signals specify bone endothelial cells during developmental osteogenesis, Nat. Cell Biol. 19 (2017) 189–201.
[29] S.K. Ramasamy, A.P. Kusumbe, M. Schiller, D. Zeuschner, M.G. Bixel, C. Milia, J. Gamrekelashvili, A. Limbourg, A. Medvinsky, M.M. Santoro, et al., Blood flow controls bone vascular function and osteogenesis, Nat. Commun. 7 (2016) 13601.
[30] S.K. Ramasamy, A.P. Kusumbe, T. Itkin, S. Gur-Cohen, T. Lapidot, R.H. Adams, Regulation of hematopoiesis and osteogenesis by blood vessel–derived signals, Annu. Rev. Cell Dev. Biol. 32 (2016) 649–675.
[31] J. Gamrekelashvili, R. Giagnorio, J. Jussofie, O. Soehnlein, J. Duchene, C. G. Briseno, S.K. Ramasamy, K. Krishnasamy, A. Limbourg, T. Kapanadze, et al., Regulation of monocyte cell fate by blood vessels mediated by Notch signalling, Nat. Commun. 7 (2016) 12597.
[32] T. Itkin, S. Gur-Cohen, J.A. Spencer, A. Schajnovitz, S.K. Ramasamy, A.P. Kusumbe, G. Ledergor, Y. Jung, I. Milo, M.G. Poulos, et al., Distinct bone marrow blood vessels differentially regulate haematopoiesis, Nature 532 (2016) 323–328.
[33] S.K. Ramasamy, A.P. Kusumbe, R.H. Adams, Regulation of tissue morphogenesis by endothelial cell-derived signals, Trends Cell Biol. 25 (2015) 148–157.
[34] C. Xu, S.S. Hasan, I. Schmidt, S.F. Rocha, M.E. Pitulescu, J. Bussmann, D. Meyen, E. Raz, R.H. Adams, A.F. Siekmann, Arteries are formed by vein-derived endothelial tip cells, Nat. Commun. 5 (2014) 5758.
[35] A.P. Kusumbe, S.K. Ramasamy, R.H. Adams, Corrigendum: coupling of angiogenesis and osteogenesis by a specific vessel subtype in bone, Nature 513 (2014) 574.
[36] H.V. Crock, A revision of the anatomy of the arteries supplying the upper end of the human femur, J. Anat. 99 (1965) 77–88.
[37] G. da Silva Feltran, R. Augusto da Silva, C.J. da Costa Fernandes, M.R. Ferreira, S. A.A. Dos Santos, L.A. Justulin Junior, L. Del Valle Sosa, W.F. Zambuzzi, Vascular smooth muscle cells exhibit elevated hypoxia-inducible Factor-1α expression in human blood vessel organoids, influencing osteogenic performance, Exp. Cell Res. 440 (2) (2024 Jul 15) 114136, https://doi.org/10.1016/j.yexcr.2024.114136. Epub 2024 Jun 22. PMID: 38909881.
[38] B. Beamer, C. Hettrich, J. Lane, Vascular endothelial growth factor: an essential component of angiogenesis and fracture healing, HSS J. 6 (2010) 85–94.
[39] H.-C. Zeng, Y. Bae, B.C. Dawson, Y. Chen, T. Bertin, E. Munivez, P.M. Campeau, J. Tao, R. Chen, B.H. Lee, MicroRNA miR-23a cluster promotes osteocyte differentiation by regulating TGF-β signalling in osteoblasts, Nat. Commun. 8 (2017) 15000.
[40] C. Bergwitz, H. Jüppner, Regulation of phosphate homeostasis by PTH, vitamin D, and FGF23, Annu. Rev. Med. 61 (2010) 91–104.
[41] J. Xiong, K. Cawley, M. Piemontese, Y. Fujiwara, H. Zhao, J.J. Goellner, C. A. O'Brien, Soluble RANKL contributes to osteoclast formation in adult mice but not ovariectomy-induced bone loss, Nat. Commun. 9 (2018) 2909.
[42] C. Greenhill, Shared variants for osteoporosis and T2DM, Nat. Rev. Endocrinol. 14 (2018) 627.
[43] W.J. Boyle, W.S. Simonet, D.L. Lacey, Osteoclast differentiation and activation, Nature 423 (2003) 337–342.
[44] P. Zhang, M. Su, S.M. Tanaka, H. Yokota, Knee loading stimulates cortical bone formation in murine femurs, BMC Musculoskelet Disord 7 (2006) 73.
[45] G.Y. Rochefort, S. Pallu, C.L. Benhamou, Osteocyte: the unrecognized side of bone tissue, Osteoporos. Int. 21 (2010) 1457–1469.
[46] S.-C. Tao, S.-C. Guo, Extracellular vesicles in bone: 'dogrobbers' in the 'eternal battle field', Cell Commun. Signal. 17 (2019) 6.
[47] R. Teo, F. Mohrlen, G. Plickert, W.A. Muller, U. Frank, An evolutionary conserved role of Wnt signaling in stem cell fate decision, Dev. Biol. 289 (2006) 91–99.
[48] T.A. Burgers, B.O. Williams, Regulation of Wnt/beta-catenin signaling within and from osteocytes, Bone 54 (2013) 244–249.
[49] E. Canalis, Wnt signalling in osteoporosis: mechanisms and novel therapeutic approaches, Nat. Rev. Endocrinol. 9 (2013) 575–583.
[50] M. Capulli, R. Paone, N. Rucci, Osteoblast and osteocyte: games without frontiers, Arch. Biochem. Biophys. 561 (2014) 3–12.
[51] J. Chen, Y. Lan, J.-A. Baek, Y. Gao, R. Jiang, Wnt/beta-catenin signaling plays an essential role in activation of odontogenic mesenchyme during early tooth development, Dev. Biol. 334 (2009) 174–185.
[52] Y. Chen, H.C. Whetstone, A.C. Lin, P. Nadesan, Q. Wei, R. Poon, B.A. Alman, Beta-catenin signaling plays a disparate role in different phases of fracture repair: implications for therapy to improve bone healing, PLoS Med. 4 (2007) e249.
[53] Y. Kitase, L. Barragan, H. Qing, S. Kondoh, J.X. Jiang, M.L. Johnson, L. F. Bonewald, Mechanical induction of PGE2 in osteocytes blocks glucocorticoid-induced apoptosis through both the beta-catenin and PKA pathways, J. Bone Miner. Res. 25 (2010) 2657–2668.
[54] X. Xia, N. Batra, Q. Shi, L.F. Bonewald, E. Sprague, J.X. Jiang, Prostaglandin promotion of osteocyte gap junction function through transcriptional regulation of connexin 43 by glycogen synthase kinase 3/beta-catenin signaling, Mol. Cell Biol. 30 (2010) 206–219.
[55] I. Kramer, C. Halleux, H. Keller, M. Pegurri, J.H. Gooi, P.B. Weber, J.Q. Feng, L. F. Bonewald, M. Kneissel, Osteocyte Wnt/beta-catenin signaling is required for normal bone homeostasis, Mol. Cell Biol. 30 (2010) 3071–3085.
[56] B. Javaheri, A.R. Stern, N. Lara, M. Dallas, H. Zhao, Y. Liu, L.F. Bonewald, M. L. Johnson, Deletion of a single beta-catenin allele in osteocytes abolishes the bone anabolic response to loading, J. Bone Miner. Res. 29 (2014) 705–715.
[57] P. Duan, L.F. Bonewald, The role of the wnt/β-catenin signaling pathway in formation and maintenance of bone and teeth, Int. J. Biochem. Cell Biol. 77 (2016) 23–29.